ELSEVIER

Journal of Applied Geophysics 49 (2002) 101–110

JOURNAL OF APPLIED GEOPHYSICS

www.elsevier.com/locate/jappgeo

Modeling confined pressure changes inducing anomalous electromagnetic fields related with earthquakes

Yukio Fujinawa [a,*], Takumi Matsumoto [a], Kozo Takahashi [b]

[a] *National Research Institute for Earth Science and Disaster Prevention, 3-1 Tennodai, Tsukuba, Ibaraki 305-0006, Japan*
[b] *Communications Research Laboratory, 4-2-1 Nukuikita, Koganei, Tokyo 184-3795, Japan*[1]

Received 4 November 1999; accepted 16 May 2000

Abstract

Electromagnetic field anomalies provide a means to estimate the confined water pressure changes through electrokinetic effects in the preparatory stages of an earthquake occurrence process. Typical shorter period pulse-like signals in the ULF band associated with seismic swarms (e.g., Fujinawa et al. [Phys. Chem. Earth (2000)]) are used to estimate the evolution of confined pressure changes based on a transient electrokinetic model. A model calculation using a simple conductivity structure indicates that the water pressure increases abruptly by several megapascals. It is indicated that sharper signals are observed at points less than a few kilometers from the source.

Keywords: Swarms; Precursor; Electric field; Electrokinetic effects; Source mechanism

1. Introduction

It is important for any candidate of precursory phenomena to be explained on a firm scientific ground in the physicochemical processes of earthquake or volcanic eruption. This step is essential in order to develop a practical and useful forecasting technique. Under this situation, we can expect a fruitful interaction between investigations on the evaluation of precursory phenomena from the standpoint of prediction and from the point of view of basic scientific interests.

A variety of anomalous electromagnetic phenomena have been studied from a practical view of prediction in a variety of frequency bands and using numerous measurement techniques (e.g., Park et al., 1993; Parrot et al., 1993; Hayakawa and Fujinawa, 1994; Hayakawa, 1999). However, the interrelation of the phenomena with earthquake occurrence has not yet been convincingly shown.

Recent accumulations of field observations and laboratory experiment as well as theoretical analyses suggest that ULF band phenomena could be induced in association with the occurrence of earthquakes and volcanic eruptions. In particular, seismic swarms are found to be accompanied by electric field anomalies of ultra-low frequency in geothermal zones (Zlotnicki and Le Mouel, 1990; Bernard, 1992; Fujinawa et al., 1992, 2000). The analysis of the data at the time of an earthquake swarm that started in August 1998 in

* Corresponding author. Tel.: +81-298-51-1611; fax: +81-298-56-2795.
E-mail address: fujinawa@bosai.go.jp (Y. Fujinawa).
[1] Former affiliation.

0926-9851/02/$ - see front matter
PII: S0926-9851(01)00102-1

central Japan provided clear evidence to show that the source was underground, and the phenomena could be explained by the electrokinetic effect (Fujinawa et al., 2000) in agreement with previous inferences (Bernard, 1992) based on observations in the active volcanic zone. In this report, we present some results of investigations on the source mechanism of ULF band electromagnetic field changes: the pressure variation inducing the anomaly.

2. Background data

The electromagnetic field has been monitored at 10 sites in the central part of Japan to evaluate the electromagnetic precursory phenomena (Fujinawa and Takahashi, 1990; Takahashi et al., 2000). Electric signals are obtained using a borehole-type underground antenna (Takahashi and Takahashi, 1989; Fujinawa and Takahashi, 1990), which provides a high S/N. We found that anomalous ULF band signals are induced at the time of seismic swarms and volcanic eruptions. Anomalous signals were recorded at Hodaka in central Japan when a seismic swarm occurred in August 1999 (Fujinawa et al., 2000; Takahashi et al., 2000), at Izu-Oshima when one of the almost periodic seismic swarms occurred off the east coast of the Izu Peninsula (Matsumoto et al., 1996), and at Awano when a recent seismic swarm occurred about 20 km northwest (Fujinawa et al., 2001). Clear signals observed at the time of a minor eruption in Izu-Oshima in 1992 (Fujinawa et al., 1992) were also very similar to those observed at the times of the seismic swarms. There are several anomalous signal waveforms of electric field in the ULF band: DC-like changes and pulse-like changes. The dominant typical signal is schematically depicted in Fig. 1. The amplitude increases abruptly, decreases gradually until about half of the peak amplitude, decreases sharply until about one-tenth of the peak, and finally returns to the gradual trend level. The magnitude of the signal measured with the use of the borehole as an ultra-long electrode (Ultra Long Electrode Measurement (ULEM)) is of the order of 100 mV.

Minor volcanic activity induced anomalies in October 1990 in Izu-Oshima, an active volcanic island, following a major eruption of Mt. Mihara in 1986. Seismic swarms occurred almost periodically from

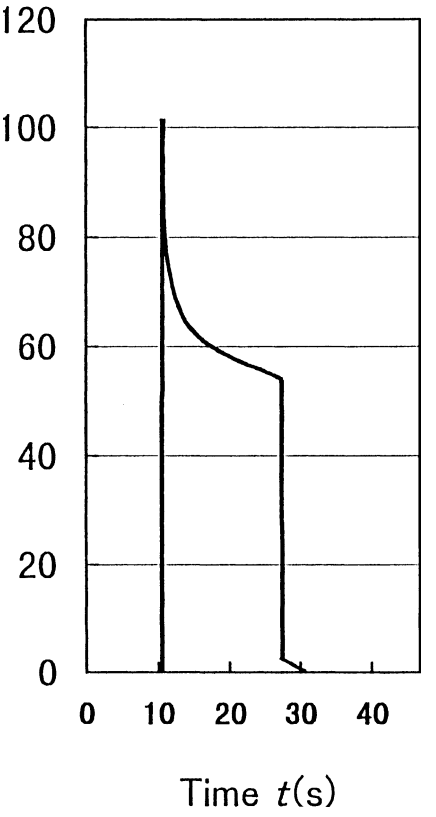

Fig. 1. A typical waveform of a higher frequency anomalous electric signal at the time of a seismic swarm and volcanic eruption. Pulse-width is from several seconds to several hundred seconds.

1979 off the east coast of the Izu Peninsula, inducing electric field anomalies, and probably caused by magma activity (e.g., Ida and Mizoue, 1991). In the northern part of the Nagano Prefecture, ULF band anomalies occurred near a famous hot spring resort and near geothermal resources. It is suggested that the last swarm activity that started in August 1998 was caused by magma movement, though there were no volcanic tremors to directly indicate magma movement (Fujinawa et al., 2000).

Our observations in central Japan cover more than 10 years and demonstrate clearly that seismic swarms and volcanic eruption are preceded by conspicuous electric field changes. It is inferred that the phenomena are related with changes of the confined water regime in the crustal activity zone (Bernard, 1992; Fujinawa et al., 2000, 2001). Here, we give a quantitative discussion based on the governing field equations.

Mizutani et al. (1976) tried to explain the observed electromagnetic anomalies associated with the Matsushiro seismic swarm on the basis of electrokinetic effects. Experimental evidence has been accumulated to indicate that a self-potential (SP) anomaly is due to electrokinetic effects (Ishido and Mizutani, 1981; Ishido and Pritchett, 1999). This situation is different from other claimed electromagnetic precursory phenomena (e.g., Park et al., 1993; Parrot et al., 1993).

The description of the electromagnetic field induced by the electrokinetic effect has been limited to stationary cases where the source region is concentrated at the boundaries of different substances (e.g., Fitterman, 1978). An extended treatment of the field calculation for a transient generating force was tried by Majaeva et al. (1997). Here, we present a reformulation suitable for wider application. A few typical field strength distributions at particular distances from the source are discussed, and observed typical signals are used to estimate confined water pressure changes by a trial and error method to explain the typical anomalous electric field waveform.

3. Formulation

Electromagnetic fields can be generated by ion transport in fluids through electrokinetic effects. The coupling between fluid motion and electric current has been described by the relation:

$$\begin{pmatrix} \boldsymbol{I}_{\mathrm{e}} \\ \\ \boldsymbol{J}_{\mathrm{f}} \end{pmatrix} = \begin{pmatrix} L_{11} & L_{12} \\ \\ L_{21} & L_{22} \end{pmatrix} \begin{pmatrix} -\nabla\phi \\ \\ -\nabla P \end{pmatrix} \tag{1}$$

where $\boldsymbol{I}_{\mathrm{e}}$ is the electric current density, $\boldsymbol{J}_{\mathrm{f}}$ is the fluid velocity, ϕ is the electric potential, P is the pore pressure, and L_{ij} is the generalized coefficient of conductivity (Overbeek, 1953; Nourbehecht, 1963; Mizutani et al., 1976; Ishido and Mizutani, 1981). Some of the coefficients are familiar electric coefficients: L_{11} is the electrical conductivity, and L_{12} is the fluid permeability of Darcy's law. The cross-coupling term containing L_{12} or L_{21} corresponds to the electrokinetic effect, with L_{12}/L_{11} being the streaming potential coefficient ($=C$) and L_{21}/L_{22} as the electro-osmosis coefficient. The generalized conductivity coefficient matrix is shown to be symmetric from Onsagar's reciprocal relations (Nourbehecht, 1963).

From Eq. (1), the electric current density $\boldsymbol{I}_{\mathrm{e}}$ is described as:

$$\boldsymbol{I}_{\mathrm{e}} = -\sigma(\nabla\phi + C\nabla P) \tag{2}$$

and the streaming potential coefficient:

$$C = \varepsilon\zeta/\sigma\mu_{\mathrm{f}} \tag{3}$$

where ζ is the zeta potential in the electric double layer formed at the solid–liquid interface, ε is the dielectric constant of the fluid, σ is the electrical conductivity, and μ_{f} is the viscosity of the fluid (Nourbehecht, 1963; Mizutani et al., 1976). This type of formulation has been adopted to explain anomalous electromagnetic field changes at the time of earthquake occurrences (Mizutani et al., 1976; Dobrovolsky et al., 1989; Fenoglio et al., 1995) and the self-potential distribution in geothermal fields (Ishido and Pritchett, 1999).

These assume a stationary state. We need a more general formulation based on Maxwell's equations for the unsteady electromagnetic field as in the case of transient field changes induced by varying pore water pressure (e.g., Fenoglio et al., 1995). Under the assumption of the quasi-stationary situation with negligible displacement current in the ordinary crustal conductive medium of piece-wise continuous continuity, Maxwell's equations are:

$$\nabla \times \boldsymbol{E} + \frac{\partial \boldsymbol{B}}{\partial t} = 0 \tag{4a}$$

$$\nabla \times \boldsymbol{H} = \boldsymbol{I}^{(\mathrm{t})} \tag{4b}$$

$$\nabla \cdot \boldsymbol{B} = 0 \tag{4c}$$

$$\nabla \cdot \boldsymbol{E} = 0 \tag{4d}$$

where $\boldsymbol{E}$ is the electric field intensity, $\boldsymbol{B}$ is the magnetic induction, $\boldsymbol{H}$ is the magnetic field intensity, and $\boldsymbol{I}^{(\mathrm{t})}$ is the total electric current density. It was shown by Nourbehecht (1963), on the basis of measurement data of Madden et al., that the electro-osmotic effect (term containing L_{21}/L_{22}) could be negligibly small compared with the hydrodynamical pressure term. In this case, it is possible to assume that the electric field is

induced by the fluid pressure gradient ∇P. Under this situation, the total electric current can be decomposed into:

$$\boldsymbol{I}^{(t)} = \boldsymbol{I} + \boldsymbol{I}^{\text{ext}} \tag{5}$$

where $\boldsymbol{I}$ is the internal current relating with the electric field intensity through a constitutive relation, and $\boldsymbol{I}^{\text{ext}}$ is the external current generated in non-electromagnetic processes (e.g., Rokityansky, 1982): in this case, a component induced by the electrokinetic effect through the pore water pressure gradient.

Additionally, we use the constitutive equations,

$$\boldsymbol{D} = \varepsilon \boldsymbol{E} \tag{6a}$$

$$\boldsymbol{B} = \mu \boldsymbol{H} \tag{6b}$$

$$\boldsymbol{I} = \sigma \boldsymbol{E} \tag{6c}$$

where μ is the magnetic permeability. The external electric current $\boldsymbol{I}^{\text{ext}}$ can be written down from (Eqs. (1), (2) and (5) as,

$$\boldsymbol{I}^{\text{ext}} = -\sigma C \nabla P \tag{7}$$

The resulting equations are the same as for the electromagnetic induction problem. Majaeva et al. (1997) derived the same result on the basis of intuitive inference that the electric current field should contain a part arising from the vector potential. Here, we have obtained the result on the basis of physical arguments.

The formulation derived for the non-stationary state has a limit in applicability because the relation of generalized velocity and thermodynamic force (Eq. (1)) are derived by assuming a steady state time invariant system. Nevertheless, we can expect that the formula will provide a useful tool to estimate the physicochemical state in the case of slowly varying systems of small flow densities (Nourbehecht, 1963).

In a piece-wise continuous medium, the electromagnetic field can be described by the following partial differential equations:

$$\left(\Delta - \frac{1}{\kappa^2}\,\frac{\partial}{\partial t}\right)\boldsymbol{F} = -\boldsymbol{\rho}(\boldsymbol{r}, t), \qquad \frac{1}{\kappa^2} = \sigma\mu \tag{8}$$

where $\boldsymbol{\rho}$ is the forcing term for the specified field quantity of interest, and $\boldsymbol{F}$ is any of electric field intensity $\boldsymbol{E}$, magnetic field intensity $\boldsymbol{H}$, or vector potential $\boldsymbol{A}$. In the case of electric field intensity $\boldsymbol{E}$, magnetic field intensity $\boldsymbol{H}$ and vector potential $\boldsymbol{A}$, $\boldsymbol{\rho}$ has the following forms:

$$\boldsymbol{F} = \boldsymbol{E}; \quad \boldsymbol{\rho}_E = -\mu \partial \boldsymbol{I}^{\text{ext}} / \partial t \tag{9a}$$

$$\boldsymbol{F} = \boldsymbol{H}; \quad \boldsymbol{\rho}_H = \nabla \times \boldsymbol{I}^{\text{ext}} \tag{9b}$$

$$\boldsymbol{F} = \boldsymbol{A}; \quad \boldsymbol{\rho}_A = \mu \boldsymbol{I}^{\text{ext}}. \tag{9c}$$

We can deduce simple characteristics of the electromagnetic field generated under the adopted assumptions from these relations. In the case of a homogeneous medium, the source term of the magnetic field intensity (Eq. (9b)) is:

$$\begin{aligned}\boldsymbol{\rho}_H &= -\sigma(\nabla C \times \nabla P + C \nabla \times \nabla P) \\ &= -\sigma(\nabla C \times \nabla P) = 0\end{aligned} \tag{10}$$

which shows that a magnetic field is not generated. It is easy to derive the source term in the case of a medium that is homogeneous except for a conductive boundary (Fitterman, 1979). As seen from Eqs. (9a),(b) and (c), there is no electric field at all for the stationary case. As for the dependence of the electromagnetic field on the medium parameters, the electric field is related to the streaming potential coefficient C, and the magnetic field to the spatial gradient of this coefficient.

Given the boundary conditions on the surrounding surface S for the domain V, the solution of Eq. (8) is:

$$\begin{aligned}\psi(\boldsymbol{r}, t) = &\int_0^t \mathrm{d}t' \int_S \mathrm{d}S' \{\boldsymbol{n} \cdot (\boldsymbol{G}\nabla' \cdot \boldsymbol{F} - \boldsymbol{F}\nabla' \cdot \boldsymbol{G}) \\ &- \boldsymbol{G} \cdot (\boldsymbol{n} \times \nabla' \times \boldsymbol{F}) - (\nabla' \times \boldsymbol{G}) \cdot (\boldsymbol{n} \times \boldsymbol{F})\} \\ &+ \int_0^t \mathrm{d}t' \int_V \boldsymbol{G}\boldsymbol{\rho}\mathrm{d}v' + \frac{1}{\kappa^2} \times \int_V \mathrm{d}v' \\ &\times \left\{\boldsymbol{G}(\boldsymbol{r}, t; \boldsymbol{r}', 0) \cdot \frac{\partial \psi(\boldsymbol{r}', 0)}{\partial t'} - \frac{\partial \boldsymbol{G}}{\partial t'} \cdot \psi(\boldsymbol{r}', 0)\right\}\end{aligned} \tag{11}$$

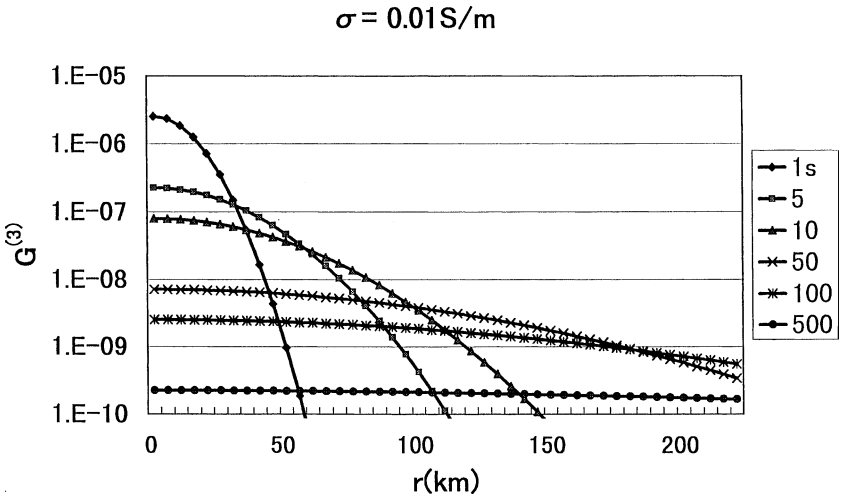

Fig. 2. Electric field strength distribution in space at several instances after the onset of a localized source at the origin ($r=0$), assuming a homogeneous medium of conductivity $\sigma=0.01$ S/m.

by the use of the tensor form of Green's function $\boldsymbol{G}(\boldsymbol{r},t|\boldsymbol{r}',t')$ satisfying the same boundary conditions,

$$\left(\Delta-\frac{1}{\kappa^2}\frac{\partial}{\partial t}\right)\boldsymbol{G}(\boldsymbol{r},t\mid\boldsymbol{r}',t') = -\delta(\boldsymbol{r}-\boldsymbol{r}')\delta(t-t') \tag{12}$$

(e.g., Morse and Feshbach, 1953), where $\boldsymbol{n}$ denotes the unit outward vector normal to the bounding surface, $\boldsymbol{\psi}(\boldsymbol{r}',0)$ the initial value of the field quantity of interest and $\boldsymbol{\rho}$ the corresponding forcing term denoted in Eqs. (9a, 9b and 9c). Then the solution $\boldsymbol{\psi}$ takes the simple form

$$\psi(\boldsymbol{r}',t)=\int_0^t \mathrm{d}t' \int_V \boldsymbol{G}\rho\, dv' \tag{13}$$

in the case of zero initial value

$$\psi(\boldsymbol{r},0)=0 \tag{14}$$

and the homogeneous boundary condition at infinite boundary. In the case of the simplest three-dimensional homogeneous medium the Green function G^3 is explicitly given as,

$$G^3(\boldsymbol{r},t;\boldsymbol{r}',t') = \frac{1}{\kappa^2}\left(\frac{1}{4\pi^2\kappa^2(t-t')}\right)^{3/2} \cdot \exp\frac{-\boldsymbol{r}\mid-\boldsymbol{r}'\mid^2}{4\kappa^2(t-t')}H(t) \tag{15}$$

when $H(t)$ is the step function,

$$H(t)=\begin{cases}0 & ; \quad t<0\\ 1 & ; \quad \geq 0\end{cases} \tag{16}$$

4. Spatio-temporal distribution of electric field

Here, we will investigate the characteristics of the electric field on the basis of the derived equations by assuming the simplest geometry of conductivity distribution. Though the uniform model seems too simple for practical application, it provides a useful clue to understand some of the general features of the electromagnetic field induced by the electrokinetic effect, such as the detectability distribution or the source mechanism giving rise to the observed electric field anomalies.

In the case of an isolated source starting at time $t=0$, the electric field is described by Green's function (Eq. (15)). The well-known form for the diffusion phenomena indicates that the electric signal is large near the source and diffuses gradually at remote points. Fig. 2 illustrates the spatial electric field distribution $G^{(3)}$ at several instances after the start of the source appearance for a uniform 3D medium with crustal conductivity $\sigma=0.01$ S/m. At the source

point, the signal decreases to less than one hundredth of the initial strength after several tens of seconds. Assuming that the relative signal detection limit corresponds to $G^{(3)}=10^{-8}$, the signal at the point $r=50$ km cannot be detected until the time $t=1$ s, then increases over the threshold limit at the time of about $t=5$ s, and then diminishes below the threshold at about $t=50$ s. That means the signal can be detected in the time interval,

$$t_s(r,\sigma) \leqq t \leqq t_e(r,\sigma) \tag{17}$$

where t_s and t_e are the start time of signal detection at distance r nearer than the detection limit r_0^e and the ending time, respectively. No signal can be detected at $r>r_0$. The maximum detection distance r_0 depends on the conductivity σ, and

$$\begin{aligned} \sigma = \quad & 0.1\ S/m; \quad r_0 \fallingdotseq 40\ \text{km} \\ & 0.01\ S/m; \quad 90\ \text{km} \\ & 0.001\ S/m; \quad 200\ \text{km} \end{aligned} \tag{18}$$

for typical values in Japan. Eq. (17) indicates that the signal detection time is different at each observation point. The values of t_e and t_s, however, are less than several tens of seconds for the conductivity ranges $\sigma=0.1-0.001$ S/m and never attain several tens of minutes under realistic crustal conductivity value. Larger retardation of the signal detection, such as that observed by our network in central Japan at the time of the Noto Peninsula Earthquake with a magnitude 6.6 in 1996, would indicate multiple sources to start signals at a different time.

The waveforms of the pulse-like signals of dominant parts of the fluctuating higher frequency component (Fig. 1) are generally characterized by a sharp increase to a peak value *Ap*, a decrease to several ten percents of the peak value, and then a gradual decrease with a duration that is almost the same as the pulse width T (several seconds to several hundred seconds) as described in more detail below:

Phase 1: initial sharp rise attaining a peak *Ap* (time constant $T_1<$ several seconds);
Phase 2: first decrease to several ten percents of Ap with time constant T_2 (several seconds $\sim 0.5T$);
Phase 3: gradual decrease with time constant T_3 (several seconds $\sim$ O(T));
Phase 4: sharp decrease to about $0.1Ap$ with time constant T_4 ($\sim T_1$); and
Phase 5: gradual decrease to the background level with time constant T_5 ($\sim 0.1T$).

The peak values *Ap* are nearly uniform over a time interval of order days except transient period of

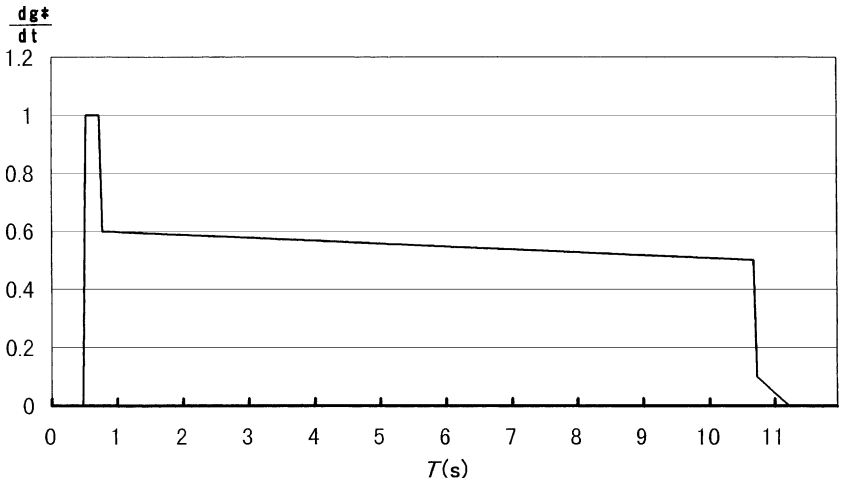

Fig. 3. Assumed rate of temporal pattern function of confined water pressure dg*/dt. (Eq. 22). Vertical axis is in arbitrary unit.

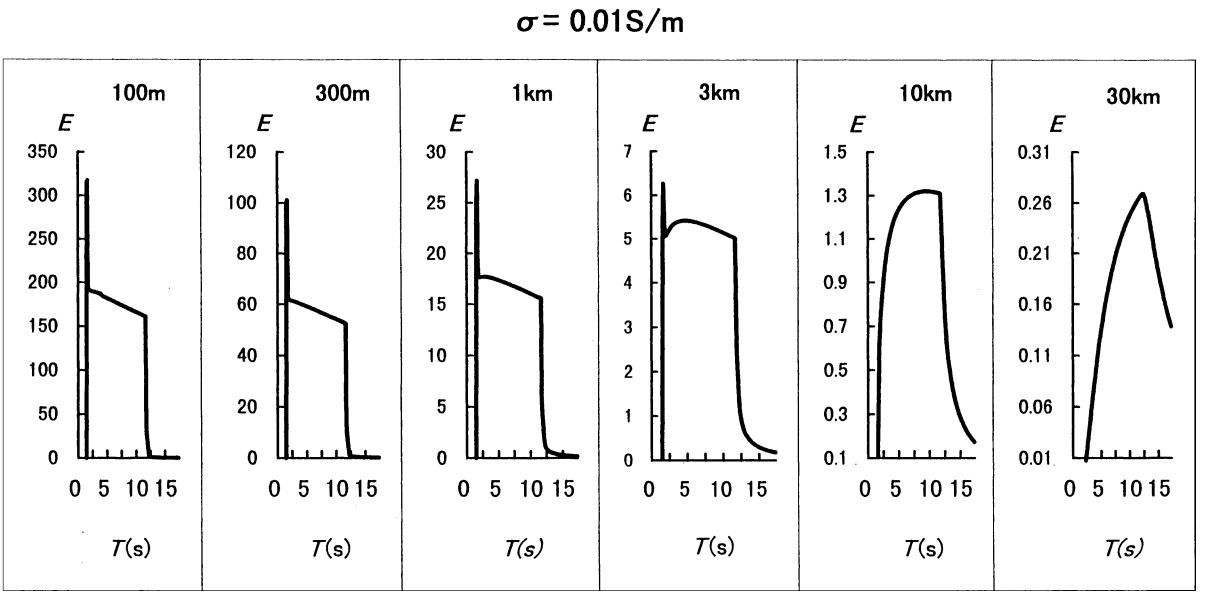

Fig. 4. Electric field strength evolution in time at several distances from the source in a homogeneous medium of $\sigma = 0.01$ S/m when the forcing term is the same as that shown in Fig. 3.

crustal activity (Takahashi et al., 2000). It is suggested that a scheme of electrokinetic interaction is preserved during that time period. The evolution of the electric field changes of the typical waveform is similar to the water pillar height change of a geyser, supporting the hypothesis that the generation mechanism of the anomalous electric field may be related to the motion of the underground flow.

We will infer that the confined pressure changes giving rise to the electric field changes under the condition of homogeneous conductivity distribution. The confined fluid pressure $P(r,t)$ is assumed for the sake of simplicity as:

$$P = P_1(r)g(t) \tag{19}$$

Then, the electric field intensity E is written down from Eq. (15),

$$E = \frac{\kappa^2}{(4\pi\kappa^2)^{3/2}}(-\mu C\nabla P_1)\tilde{g}\cdot\int_0^t \mathrm{d}t_0 \frac{\mathrm{d}g^*}{\mathrm{d}t}(t_0) \times \frac{\mathrm{e}^{-r^2/(4\pi\kappa^2(t-t_0))}}{(t-t_0)^{3/2}}H(t-t_0) \tag{20}$$

where the temporal part $g(t)$ is decomposed by defining a scaling factor $\tilde{g}$ and temporal pattern function $g^*(t)$:

$$g(t) = \tilde{g}\cdot g^*(t) \tag{21}$$

As an example, the electric field intensity E in the direction of the pressure gradient is calculated by taking $\tilde{g} = 1$ and $g^*(t)$ as (Fig. 3) for $\sigma = 0.01$ S/m,

$$\begin{aligned} g^*(t) &= 0, && t < 0 \\ &= 10, && 0 \leqq t < 0.25 \\ &= 0.6\sim 0.5, && 0.25 \leqq t < 10.25 \\ &= 0.5\sim 0, && 10.25 < t \leqq 10.75 \end{aligned} \tag{22}$$

Fig. 4 shows that the resulting time evolution of the electric field E at several distances from the source. Units of the electric field intensity E are in millivolts with the choice of model parameters of $\varsigma = 0.1$ V, $|\nabla P| = 4$ MPa, $\varepsilon = 8\varepsilon_0$ (ε_0 is the dielectric constant in free space) and the source volume of 800 m^3. The choice of the values for zeta potential and the pressure

gradient rely on the discussion of Fenoglio et al. (1995). The homogeneous source volume was determined for the electric field to be in agreement with the observed value by assuming that a part of the electrodes with a length of 100 m is exposed to the field. The temporal changes are similar to each other at points near the source: phase 1 and phase 2 with a sharp change are reproduced in the near field at a distance less than 3 km. However, the signal is diffused sufficiently at several kilometers away from the source to lose the sharpness of the driving force. It is seen that the signal deformation increases with the distance from the source and that amplitude decreases rapidly. In other words, the signal waveform conveys information about the source distance. The detection of the similarly sharp anomalous electric field changes suggests that the confined water pressure increases sharply in the initial phases in the process of conspicuous and rapid changes of hydrothermal circulation. We can infer that the typical anomalies observed by the borehole antenna at the time of crustal activities were detected only near the source. The amplitude ratio of main phase 3 to the peak value is also conserved in the near field, but decreases rapidly in the far field. The electric field strength E decreases as $E \sim 1/r$ in the distance interval 100 m–10 km in the case indicated in Fig. 4.

We can calculate the signal waveform if the source function and the conductivity distribution are given. But usually, we want to infer those unknowns as an inverse problem using the observed data. Source parameters of earthquakes are now routinely determined using seismic observation data on the earth's surface. One of the unknowns, the seismic velocity, is generally assumed to be known from the seismic survey, and the source time function describing the fault motion is estimated by use of the seismic waveform observation at multiple sites (Aki and Richards, 1980). A similar approach could be taken in the field of research of the present interest as a kind of future problem.

The conductivity structure is determined by an electromagnetic induction survey (Rokityansky, 1982) though the profile is not as elaborately known as the seismic velocity profile. Observed electric signals at multiple sites can be used to determine the source position and the source time function if we have enough knowledge about the detailed conductivity distribution as recently observed in the central part of the northeastern part of Japan (Fujinawa et al., 1999).

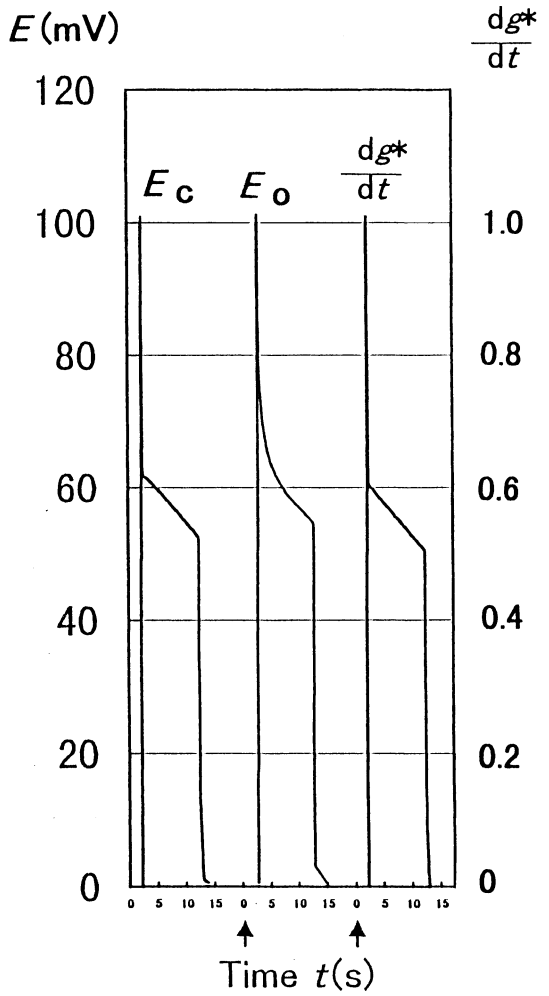

Fig. 5. The units for the observed electric field E_o and for the synthetic field E_c is shown on the left side, and the unit for the source time function is shown on the right side.

The rate of the pressure change shown in Fig. 5a $\left(\frac{dg^*}{dt}\right)$ has been obtained to model the observed typical electric signals shown in the same figure (Ec) by a trail and error method. The calculated field Ec refers to $r = 300$ m using conductivity $\sigma = 0.01$ S/m. At near field, there is a large degree of similarity between the waveform of the source function and the synthetic curve. The minor discrepancy in the synthetic waveform compared with the observed one would be

reduced by choosing a slightly different source function g^* compared with the term shown in Fig. 3. In principle, we can calculate the source time function g^* from the observed signals if we have enough knowledge of the conductivity distribution and relevant parameters just as in the analysis of seismic fault mechanisms.

5. Discussion

Typical signals in the anomalous electric field changes indicate that the rate of the confined pressure changes is dominantly positive. Our observations show that there is a short time period when the polarity of the signals is negative. There must be a persistent increase or decrease of the confined pressure during these time periods. The longer period components of the pressure changes corresponding to the DC-like electric signals (Fujinawa et al., 2000) may more or less compensate the accumulated increase or decrease induced by a considerable number of the higher frequency components.

Electric field anomalies were also observed in Greece (Varotsos et al., 1996) and in Japan (Nagao et al., 1996) for the case of main shock–aftershock-type events. These signals had longer period and occurred at a much shorter time interval than those discussed here. We could interpret the longer period feature of their results on the basis of the extinction of the higher frequency components at remote points as suggested from the dependence of signal waveform on distance (Fig. 4).

From the observational point of view, a sensor buried deep under the ground near the source could provide us with the possibility to detect even a small signal induced by confined water pressure change. Moreover, the extraordinary long distance detectability as claimed in Greece amounting to several tens of the rupture area could be understood, if it is not artificial noise, as due to the installment of the sensor near the ground surface where the signal strength is large enough owing to the shorter distance from the signal source. We can assume that the area is well connected to the seismic zone through a ground water conduit. However, the existences of such a conduit needs to be shown by high-resolution studies (Varotsos et al., 1996).

Acknowledgements

We would like to express our thanks to many individuals, institutes and organizations which have extended considerable help in the undertaking of this work, especially to Dr. Hiroshi Takahashi, Dr. Yukio Hagiwara, Dr. Shigetsugu Uyehara, Dr. Tsuneo Ishido and Dr. Hiroshi Iitaka. Careful readings of the original manuscript by Prof. Seiya Uyeda and an anonymous reviewer are greatly acknowledged. We are grateful to Mr. Wu Yeu Sheng and Ms. Yumiko Yamauchi for their assistance in the preparation of the manuscript.

References

Aki, K., Richards, P.G., 1980. Quantitative Seismology — Theory and Methods. Freeman, San Francisco, 932 pp.

Bernard, P., 1992. Plausibility of long distance electrotelluric precursors to earthquakes. J. Geophys. Res. 97, 17531–17546.

Dobrovolsky, I.P., Gershenzon, N.I., Gokhberg, M.B., 1989. Theory of electrokinetic effects occurring at the final stage in the preparation of a tectonic earthquake. Phys. Earth Planet. Inter. 57, l44–l56.

Fenoglio, M.A., Johnston, M.J.S., Byerlee, J.D., 1995. Magnetic and electric fields associated with changes in high pore pressure in fault zones: application to the Loma Prieta ULF emissions. J. Geophys. Res. 100, 12951–12958.

Fitterman, D.V., 1978. Electrokinetic and magnetic anomalies associated with dilatant regions in a layered earth. J. Geophys. Res. 83, 5923–5928.

Fitterman, D., 1979. Calculations of self-potential anomalies near vertical contacts. Geophysics 44, 195–205.

Fujinawa, Y., Takahashi, K., 1990. Emission of electromagnetic radiation preceding the Ito seismic swarm of 1989. Nature 347, 376–378.

Fujinawa, Y., Takahashi, K., Kumagai, T., 1992. A study of anomalous underground electric field variations associated with a volcanic eruption. Geophys. Res. Lett. 19, 9–12.

Fujinawa, Y., Kawakami, N., Inoue, J., Theodore, H.A., Takasugi, S., Honkura, Y., 1999. 2-D georesistivity structure in the central part of the northeastern Japan arc. Earth Planets Space 51, 1035–1046.

Fujinawa, Y., Takahashi, K., Matsumoto, T., Iitaka, H., Yamane, S., Nakayama, T., Sawada, T., Sakai, H., 2000. Electromagnetic field anomaly associated with the 1998 seismic swarm in central Japan. Phys. Chem. Earth 25, 247–253.

Fujinawa, Y., Takahashi, K., Matsumoto, T., Iitaka, H., Yamane, S., Nakayama, T., Sawada, T., Sakai, H., 2001. Characteristics of electromagnetic field changes related to earthquakes swarms. Bull. Earthquake Research Inst. (in press).

Hayakawa, M. (Ed.), 1999. Atmospheric and Ionospheric Electromagnetic Phenomena Associated with Earthquake. Terra Scientific Pub., Tokyo, p. 996.

Hayakawa, M., Fujinawa, Y., 1994. Electromagnetic Phenomena Related to Earthquake Prediction. Terra Scientific Pub., Tokyo, 677 pp.

Ida, Y., Mizoue, M., 1991. Seismic and volcanic activity in around the Izu Peninsula and its tectonic implications. J. Phys. Earth 39 (1), 1–460.

Ishido, T., Mizutani, H., 1981. Experimental and theoretical basis of electrokinetic phenomena in rock–water systems and its applications to geophysics. J. Geophys. Res. 86, 1763–1775.

Ishido, T., Pritchett, J.W., 1999. Numerical simulation of electrotelluric potentials associated with subsurface florid flow. Geophys. Res. Lett. 104, 15247–15259.

Majaeva, O., Fujinawa, Y., Zhitomirsky, M.E., 1997. Modeling of non-stationary electrokinetic effect in a conductive crust. J. Geomagn. Geoelectr. 49, 1317–1326.

Matsumoto, T., Fujinawa, Y., Takahashi, K., 1996. ULF-bands electric field changes related to seismic swarms. J. Atmos. Electr. 16, 175–191.

Morse, P.M., Feshbach, H., 1953. Methods of Theoretical Physics, Part 1. McGraw-Hill, Tokyo.

Mizutani, H., Ishido, T., Yokokura, T., Ohnishi, S., 1976. Electrokinetic phenomena associated with earthquakes. Geophys. Res. Lett. 3, 365–368.

Nagao, T., Uyeda, S., Asai, Y., Kono, Y., 1996. Anomalous changes in geoelectric potential preceding four earthquakes in Japan. In: Lighthill, J. (Ed.), A Critical Review of Van. World Scientific Pub., pp. 292–300.

Nourbehecht, B., 1963. Irreversible Thermodynamic Effects in Inhomogeneous Media and Their Applications in Certain Geoelectric Problems. Mass. Inst. of Technol., Cambridge, MA.

Overbeek, J.T., 1953. Thermodynamics of electrokinetic phenomena. J. Colloid Sci. 8, 420.

Park, S.K., Johnston, M.J.S., Madden, T.R., Morgan, F.D., Morrison, F., 1993. Electromagnetic precursors to earthquake in the ULF band: a review of observations and mechanisms. Rev. Geophys. 31, 117–132.

Parrot, M., Achache, J., Berthelier, J.J., Blanc, E., Deschamps, A., Lefeuvre, F., Menvielle, M., Plantet, J.L., Tarits, P., Villain, J.P., 1993. High-frequency seismo-electromagnetic effects. Phys. Earth Planet. Inter. 77, 65–83.

Rokityansky, I.I., 1982. Geoelectromagnetic Investigation of the Earth's Crust and Mantle. Springer-Verlag, Berlin.

Takahashi, H., Takahashi, K., 1989. Tomography of seismo-radio wave source regions for predicting imminent earthquakes. Phys. Earth Planet. Inter. 51, 40–44.

Takahashi, H., Fujinawa, Y., Matsumoto, T., Nakayama, T., Sawada, T., Sakai, H., Iitaka, H., 2000. An anomalous electric field variation associated with the seismic swarm (1) — Underground electric field observation at Hodaka Station — (1993–1999). Report of National Research Institute for Earth Science and Disaster Prevention, 2000, 1–224.

Varotsos, P., Lazaridou, M., Eftaxias, K., Antonopoulos, G., Makris, J., Kopanas, J., 1996. Short-term earthquake prediction in Greece by seismic electric signals. In: Lighthill, J. (Ed.), A Critical Review of VAN. World Science Publishing, Singapore, pp. 29–76.

Zlotnicki, J., Le Mouel, J.L., 1990. Possible electrokinetic origin of large magnetic variations at La Fournaise Volcano. Nature 343, 633–636.